JOURNAL OF CATALYSIS 76, 320–332 (1982)

Oxidation States of Copper on Alumina Studied by Redox Cycles

M. LO JACONO, A. CIMINO,[1] AND M. INVERSI

Centro di Studio S.A.C.S.O. (C.N.R.), Istituto di Chimica Generale ed Inorganica, Università di Roma, 00100 Rome, Italy

Received August 19, 1981; revised February 26, 1982

Supported copper oxide on γ-alumina (2,4, or 10% Cu atoms per 100 Al) was subjected to cycles of reduction (by hydrogen) and oxidation (by oxygen). From the hydrogen consumed, from the water released, and from the oxygen used in the oxidation step it was possible to deduce the molar fractions of Cu^0, Cu^{1+}, and Cu^{2+} present, as a function of the extent of reduction. At low copper loadings (2 or 4%) Cu^{1+} is preferentially formed. The reduction to Cu^0 is thermodynamically favorable, but kinetically hindered. The role of the support and of the surface configuration is discussed.

INTRODUCTION

The interest in copper-containing catalysts has prompted several studies of the copper-on-alumina system (*1, 2*). Several techniques have been employed to elucidate the state of the copper ions (oxidation number, dispersion), the interaction with the support, and the ensuing variation of redox properties. The last aspect, redox properties, is of particular importance since copper-containing catalysts can be used in a variety of atmospheres, and catalytic activity has been sometimes ascribed to a particular oxidation state (*3*). One way of obtaining direct chemical information on the oxidation state of copper is to subject the catalyst to redox cycles in hydrogen and oxygen and then titrate thereby deducing the average oxidation number. Moreover, if reasonable assumptions are adopted, as successfully shown in the case of the MoO_3/Al_2O_3 system (*4*), the mole fractions of Cu^{2+}, Cu^{1+}, and Cu^0 can be deduced.

At low copper loadings, the Cu^{2+}/Al_2O_3 system, which constitutes our starting system, has been shown to consist of a dispersion of copper ions forming, on the surface of the alumina, a structure related to that of the spinel $CuAl_2O_4$, and hereafter called "surface spinel." Most of the Cu^{2+} ions are in a distorted octahedral geometry unlike the bulk $CuAl_2O_4$ where about 60% is in a tetrahedral geometry (*5a, b*). An appraisal of earlier work and a discussion of the picture emerging from a variety of techniques are given by Friedman *et al.* (*1*), to whom reference will be made below. It is in particular recalled that if the loading exceeds about 4 Cu percent by weight per 100 $m^2 g^{-1}$ of the support, the oxide CuO is present.

EXPERIMENTAL

1. Catalyst Preparation and Characterization

The γ-Al_2O_3 support was prepared according to the method described by McIver *et al.* (*6*). The copper-containing catalysts were prepared by impregnation of the alumina with a comparable volume of a titrated solution of copper nitrate (C. Erba, reagent grade). The soaked paste was dried at 120°C, ground, and calcined at 600°C in air for 24 h. The specimens are designated as $A_\gamma Cu\ x$, where x indicates the nominal copper content (Cu atoms per 100 Al atoms). The catalysts, and their features, are listed in Table 1.

The copper-containing catalysts were

[1] To whom correspondence should be addressed.

0021-9517/82/080320-13$02.00/0

TABLE 1

Specimens and Their Properties

Sample	Cu content (% by weight)[a]	μ_{eff}[b] (B.M.)	θ[b] (K)	Phases (x ray)	Cu^{2+} symmetry[c]
$A_\gamma Cu$ 1	1.36	1.91		γ-Al_2O_3	O
$A_\gamma Cu$ 1.5	2.03	1.96		γ-Al_2O_3	O
$A_\gamma Cu$ 2	2.67	1.91		γ-Al_2O_3	O
$A_\gamma Cu$ 3	3.87	2.00	−20	γ-Al_2O_3, $CuAl_2O_4$[d]	O
$A_\gamma Cu$ 4	5.05	1.90	−17	γ-Al_2O_3, $CuAl_2O_4$[d]	O
$A_\gamma Cu$ 5	6.35	1.90	−17	γ-Al_2O_3, $CuAl_2O_4$[d]	O
$A_\gamma Cu$ 10	11.48	1.92	−34	γ-Al_2O_3, $CuAl_2O_4$[d]	O
$A_\gamma Cu$ 20	19.92	1.52	−58	γ-Al_2O_3, $CuAl_2O_4$[d], CuO	O
$A_\gamma Cu$[e] 20	21.40	2.33	−190	$CuAl_2O_4$[f], α-Al_2O_3	T

[a] Analytical content.
[b] μ_{eff} and θ are the effective magnetic moment and the Weiss temperature; see text.
[c] Dominating symmetry (see text): O = octahedral, T = tetrahedral.
[d] Incipient "surface spinel."
[e] Sample fired at 900°C.
[f] Bulk spinel.

characterized by the following techniques:

(a) chemical analysis by atomic absorption;

(b) X-ray analysis with a Debye–Scherrer camera or counter diffractometer ($CuK\alpha$ radiation) for phase identification;

(c) diffuse reflectance spectroscopy by means of a Beckman DK1 spectrophotometer, using γ-Al_2O_3 or MgO as reference (wavelength range 2500 to 250 nm);

(d) magnetic susceptibility by the Gouy method, in the range 100 to 300 K.

2. *Redox Cycles*

The reduction–oxidation cycles were performed in a BET-type vacuum line. The volume of gases consumed was determined by measurement of pressure variations (error ± 0.05 Torr). The system was provided with a magnetically driven glass pump. The techniques and procedures were those reported by Hall and co-workers (*4*, *7*). The sample (1 or 2 g) was pretreated in flowing dry O_2 overnight at 500°C, followed by evacuation at 500°C for 20 min before the redox cycle started.

The first step of the cycle (reduction) involved treatment at a given temperature with a known amount of hydrogen previously purified over magnesium perchlorate and activated charcoal at 78 K. The gas was circulated through the catalyst and through a cold trap (78 K). The total hydrogen consumed $(H_2)_c$, was measured by the drop in pressure. At the end of the reduction, the hydrogen gas was removed through the cold trap, and evacuation continued for 1 to 1.5 h at 450°C. In some cases, the evacuation was carried out at the same temperature as reduction (100 to 200°C) to avoid sintering. The last procedure was adopted when the Cu metal was titrated with N_2O at room temperature (r.t.). The water released in the process, $(H_2O)_R$, and collected in the trap was then measured after successive expansions into the BET system, care being taken to maintain the vapor pressure well below condensation. The second step (oxidation) consisted in a treatment at 450°C with a known amount of O_2 (doubly distilled) circulated over the catalyst for 40 to 60 min and through a cold trap (195 K). The oxygen consumption $(O_2)_c$ was thereby measured. In some instances the oxidation step followed a titration of Cu^0 by N_2O (see below). In Section 4 (Treatment of Data)

the implication of this N_2O step will be specified.

After each cycle, the catalyst was regenerated by flowing O_2 at 500°C overnight, and the cycle could be repeated.

3. Titration of Cu^0 by N_2O

The N_2O (doubly distilled) circulated over the catalyst for 20 min at r.t. The N_2 resulting from the decomposition (N_2) was measured after freezing the undecomposed N_2O at 78 K. The method (*8*) titrates the exposed copper atoms, and gives the total copper content only if the metal is well dispersed. This condition is achieved at low extent of reduction and at low (4 at.%) copper content, by evacuating the catalyst at the same temperature of reduction (100 or 200°C). With this procedure, it was found that the Cu^0 thereby determined agrees with that calculated *via* the water released in step 1, $(H_2O)_R$.

4. Treatment of Data

From the quantities measured during the first and the second steps of the redox cycle it is possible to calculate the amount of relevant surface species on the basis of mass balance equations. The different quantities are essentially defined according to Hall and Massoth (*7*) for the MoO_3/Al_2O_3 system, with some change in symbolism, and expressing in each case in parentheses the number of moles. In view of the fundamental role of the quantities in discussion, their definition is briefly reviewed. The quantities $(H_2)_c$ (hydrogen consumed) and $(H_2O)_R$ (water released), were operationally defined before. The quantity $(H_2)_I$ (irreversible hydrogen) is the hydrogen retained by the catalyst even after pumping out at 450°C, whilst $(H_2)_R$ (reversible) is the amount desorbed during the evacuation process. The first mass balance equation for the reduction step can thus be written

$$(H_2)_c = (H_2O)_R + (H_2)_I + (H_2)_R. \quad (1)$$

A substantial portion of the hydrogen consumed does not appear as water released but is either pumped off after adsorption or irreversibly held. The H_{2_I} species is believed to be present as OH^- groups; hence each hydrogen atom reduces the surface by 1 eq.

The following equations can be representative of the chemistry involved (only the oxidation state of copper is specified, and H_I indicates the irreversible hydrogen):

$$2Cu^{2+}Al_2O_4 + H_2 \rightarrow 2Cu^{1+}Al_2O_3OH_I, \quad (a)$$

$$Cu^{2+}Al_2O_4 + H_2 \rightarrow Cu^0 + Al_2O_3 + H_2O. \quad (b)$$

The second mass balance equation is derived from the oxidation step, the chemistry of which can be written as

$$2Cu^{1+}Al_2O_3OH_I + \tfrac{1}{2}O_2 \rightarrow 2CuAl_2O_4 + H_2O, \quad (c)$$

$$Cu^0 + Al_2O_3 + \tfrac{1}{2}O_2 \rightarrow CuAl_2O_4. \quad (d)$$

In the oxidation steps, therefore, the oxygen mass balance is made up by the sum of two terms: the oxygen retained by the catalyst plus the water released. The first term, oxygen retained (Eq. (d)), replenishes the oxygen lost as water in the reduction step, and is therefore given by $(H_2O)_R$. The second term, water released, originates from the oxidation of (reduced) species bound to OH^- ions (Eq. (c)). From inspection of the stoichiometry of Eqs. (a) to (d) the mass balance equation is then

$$2(O_2)_c = (H_2O)_R + (H_2)_I. \quad (2)$$

It should be noted that the total reduction cannot be evaluated by $(H_2O)_R$ alone, because of the presence of irreversible hydrogen, as already noted by Hall and Lo Jacono for the MoO_3/Al_2O_3 system (*4*). It should be further noted that there is the implicit assumption that the state of hydroxylation of the surface is reproduced at the end of each cycle.

The extent of reduction e/Cu is defined as the ratio between the number of hydrogen equivalents consumed for the reduction process given by $2(H_2O)_R + 2(H_2)_I$ and the

TABLE 2

Redox Cycles on Copper–Alumina Catalysts

Catalyst and Expt. No.	Reduction step					N_2O	Oxidation step			Eq ratio[e]	e/Cu[f]
	Temp. (°C)	Time (min)	Final pressure (Torr)	V_H[a] (cm^3, NTP)	V_W[b]	V_N[c]	Time (min)	Final pressure (Torr)	V_o[d]		
$A_\gamma Cu$ 2											
1	200	75	561	2.30		0.21	60	327	1.10	1.04	0.24
2	500	55	482	14.97	9.4		60	264	7.08	0.95	1.50
4	200	100	436	3.88		0.29	60	154	1.80	1.00	0.41
5	250	45	382	6.55		0.72	80	127	2.71	0.94	0.65
6	300	70	326	10.71		1.32	40	92	4.7	1.00	1.14
7	500	60	274	14.61	9.95		60	56	7.28	1.00	1.55
$A_\gamma Cu$ 4											
2	100	120	366	3.40	(0.36)		40	370	1.60	0.94	0.18
3	100	130	392	4.27	(0.54)		40	380	1.98	0.93	0.27
4	200	60	350	13.75		1.54					0.77
6	250	120	415	23.75		3.12	40	382	9.60	0.94	1.26
7	250	60	365	22.08	5.31		60	398	10.47	0.95	1.18
11	500	40	500	27.34	16.09		60	340	13.00	0.95	1.46
12	500	150	600	28.65	20.60		45	330	14.30	1.00	1.61
13	200	80	521	20.29		2.40	60	324	8.50	0.96	1.10
$A_\gamma Cu$ 10											
5	100	60	646	18.85	10.83		60	349	8.61	0.92	0.85
6	100	60	518	15.46	10.96		60	288	7.94	1.03	0.78
7	100	20	294	10.36	6.49		60	435	5.00	0.96	0.51
8	100	60	628	20.1	12.75		60	413	9.29	0.93	0.92
9	200	60	474	27.72	18.07		60	415	14.07	1.01	1.39
10	300	60	595	29.59	18.64		60	378	14.77	1.00	1.46
11	400	60	621	31.32	20.86		60	486	15.96	1.02	1.58
12	500	60	652	32.6	27.81		60	516	16.24	1.03	1.66
3[g]	500	60	261	34.6	28.05		60	512	17.2	0.99	1.71

[a] V_H = Total volume of hydrogen consumed, H_{2_c}, at NTP (amounts used: $A_\gamma Cu$ 2 and $A_\gamma Cu$ 4, 2 g; $A_\gamma Cu$ 10, 1 g).
[b] V_W = Volume of H_2O released, H_2O_R, at NTP.
[c] V_N = Volume of N_2 released after N_2O titration, at NTP.
[d] V_o = Volume of oxygen consumed, O_{2_c}, at NTP.
[e] Ratio (oxygen equivalents)/(hydrogen equivalents). The equivalents are calculated as specified in the text.
[f] e/Cu extent of reduction, see text.
[g] New portion of $A_\gamma Cu$ 10.

No. of Cu atoms. From Eq. (2), the number of hydrogen equivalents is therefore also given by $4(O_2)_c$. It was possible to check the internal consistency of the data by checking the ratio (unity in principle) between the equivalents of hydrogen and the equivalents of oxygen (Table 2). However, when a titration with N_2O was carried out, the equivalents of oxygen left on Cu^0 by the titration, $2(N_2)$, was also taken into account. Accordingly, the amount $2(N_2)$ was added to the equivalents $(4(O_2)_c)$.

RESULTS

1. *Characterization of Oxidized Catalyst*

X-ray. The X-ray pattern of copper-containing samples was similar to that of γ-Al_2O_3. This is not unexpected since γ-Al_2O_3 has a defect spinel structure with a close-packed oxygen lattice very similar to that of $CuAl_2O_4$. It is possible, however, to detect the incipient formation of the "surface spinel," if attention is focused on the intensity behavior of diffraction lines at $d = 2.8$ and 2.4 Å. The intensity of these two lines, which are strong lines for the spinels, increases with copper content, as found for the Ni^{2+}/Al_2O_3 system (*9*). The specimen $A_\gamma Cu$ 20 calcined at 600°C showed the presence of CuO bulk phase whereas the same sample calcined at 900°C contains the spinel $CuAl_2O_4$ phase and α-Al_2O_3.

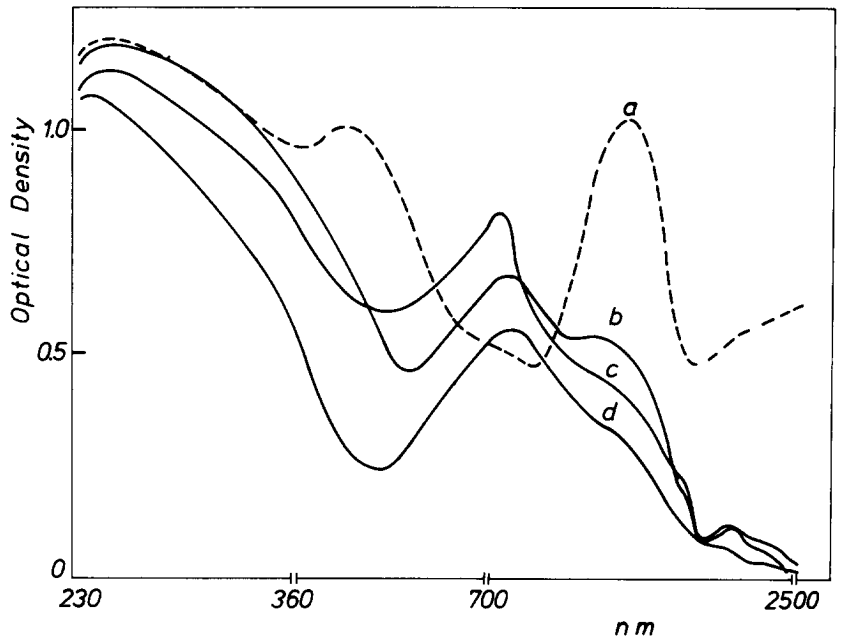

FIG. 1. Reflectance spectra of Cu^{2+}/γ-Al_2O_3 samples: (a) $A_\gamma Cu$ 20 (900°C); (b) $A_\gamma Cu$ 10; (c) $A_\gamma Cu$ 20; (d) $A_\gamma Cu$ 4.

Reflectance spectra. The copper-containing samples show two typical absorption bands due to Cu^{2+} ions in octahedral and in tetrahedral symmetry, with the maxima located respectively in the absorption regions between 1400–1600 and 750–850 nm (Fig. 1).

The octahedral absorption band, due to the spin-allowed transition $^2E_g \rightarrow {}^2T_{2g}$, dominates the spectrum for specimens calcined at 600°C. The band is very intense and rather symmetric as compared to the very weak tetrahedral band, due to the transition $^2T \rightarrow {}^2E$. By recalling that the extinction coefficient for tetrahedral bands is roughly 10–100 times that for octahedral bands it can be deduced that about 98% of the cupric ions are located at the octahedral sites. It should be noted that the octahedral peak becomes asymmetric at the high-energy side for the sample $A_\gamma Cu$ 10. This result points to the incipient segregation of the CuO phase, which becomes quite visible in the $A_\gamma Cu$ 20 (600°C) spectrum. Finally, in agreement with literature data (*10*) the reflectance spectrum of $A_\gamma Cu$ 20 (900°C) shows only the tetrahedral peak of Cu^{2+} ions, due to the low extinction coefficient of the octahedral ions.

Magnetic susceptibility. The experimental effective magnetic moment, μ_{eff}, and the Weiss temperature, θ, obtained from the plots of χ^{-1} vs T were 1.9 B.M. and −20 K, respectively, for the samples calcined at 600°C (Table 1). Only the specimen $A_\gamma Cu$ 20 (600°C) showed a magnetic moment of 1.5 B.M. and Weiss temperature of −60 K, a result which reflects and confirms the presence of the antiferromagnetic CuO phase (*18*).

As far as the $A_\gamma Cu$ 20 calcined at 900°C is concerned the higher values of μ_{eff} and of θ confirm the presence of the bulk-phase $CuAl_2O_4$ (*5b*).

2. Redox Cycles

Table 2 lists the measured quantities $(H_2)_c$, $(H_2O)_R$, (N_2), and $(O_2)_c$ for the specimens $A_\gamma Cu$ 2, $A_\gamma Cu$ 4 (amount used 2 g), and $A_\gamma Cu$ 10 (amount used 1 g). In analogy with the molybdena–alumina system, it is assumed that the amount of Cu^0 produced is

measured by the water released $(H_2O)_R$, and the amount of Cu^{1+} is measured by $(H_2)_I$. The amount of Cu^0 can also be measured by the N_2O titration method thereby providing an independent check. On these grounds, it is possible to extract the molar fraction of each species, Cu^{2+}, Cu^{1+}, and Cu^0, as a function of the extent of reduction e/Cu. It should be noted that in order to achieve increasing e/Cu values, the reduction temperature is increased (see Table 2).

The results for $A_\gamma Cu$ 2 and $A_\gamma Cu$ 4 are shown in Fig. 2. It can be noted first that the molar distribution of Cu^{2+}, Cu^{1+}, and Cu^0 for these two specimens is independent of copper content, and second, that in the range $e/Cu \leq 1.2$ both Cu^{1+} and Cu^0 vary linearly with e/Cu. The ratio Cu^{1+}/Cu^0 produced is about 4. The complete disappearance of Cu^{2+} takes place at about $e/Cu = 1.2$. Titration of Cu^0 by N_2O gives values in good agreement with those calculated for $(H_2O)_R$ except when sintering takes place. In this case, only a fraction of copper atoms is titrated by N_2O. The amount of Cu^{1+}, which is deduced from the amount of hydrogen consumed and from the N_2O titration, is thereby overestimated. As an example, a specimen $A_\gamma Cu$ 4 reduced at 300°C, gave rise to a Cu^0 content (from N_2O) of 18.5% and to a Cu^{1+} content of 92%. Clearly the sum (110.5%) exceeds the experimental error of evaluation of volumes, and the discrepancy is solely due to the incorrect assumption that all Cu^0 is titrated by N_2O. In this case, if N_2O reacts at high temperatures the amount of N_2 produced increases, but it becomes difficult to discriminate the stoichiometric reaction from sustained catalytic decomposition.

The case of $A_\gamma Cu$ 10 is now examined (Fig. 3). For this specimen, which contains CuO, some difficulty was experienced in obtaining a good reproducibility, except after a few cycles. For comparison, in the same figure the data obtained for $A_\gamma Cu$ 2 and $A_\gamma Cu$ 4 are reported as broken lines. The most striking feature in the range $0 < e/Cu < 1.5$ is the greater amount of Cu^0, and lower amount of Cu^{1+}, when compared with

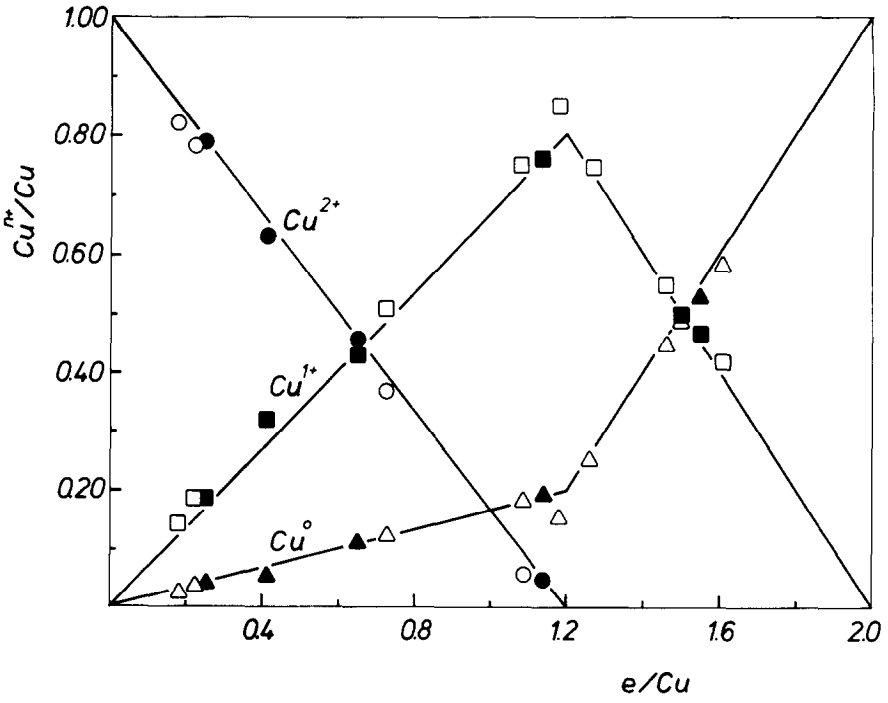

FIG. 2. Molar fraction Cu^{n+}/Cu (n = 0, 1, 2) vs extent of reduction e/Cu: ○, ●, Cu^{2+}/Cu; □, ■, Cu^{1+}/Cu; △, ▲, Cu^0/Cu. Solid symbols, $A_\gamma Cu$ 2; open symbols, $A_\gamma Cu$ 4.

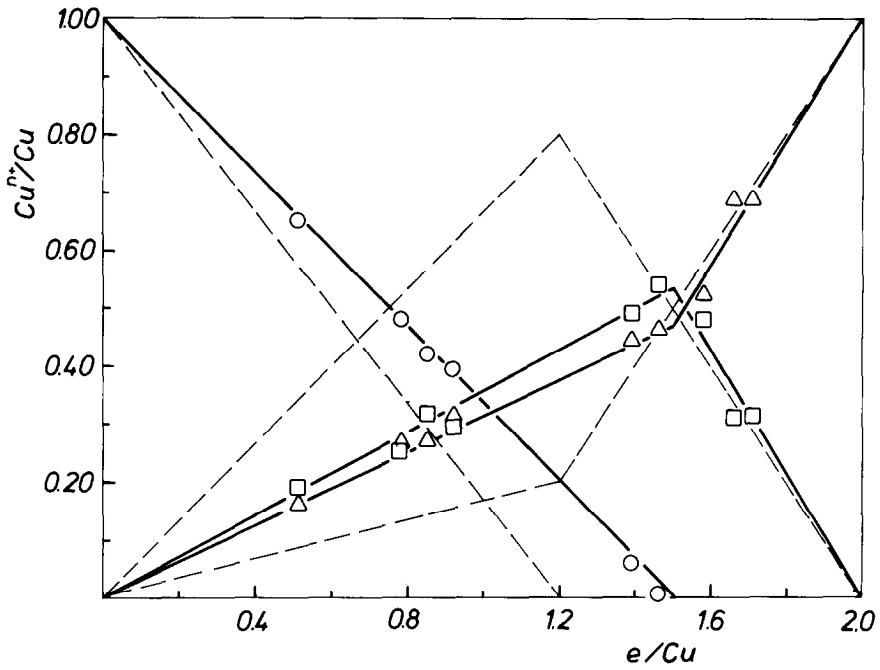

FIG. 3. Molar fraction Cu^{n+}/Cu (n = 0, 1, 2) vs extent of reduction e/Cu for $A_\gamma Cu$ 10: ○, Cu^{2+}/Cu; □, Cu^{1+}/Cu; △, Cu^0/Cu. The broken lines refer to samples $A_\gamma Cu$ 2 and $A_\gamma Cu$ 4 (Fig. 2).

$A_\gamma Cu$ 2 and $A_\gamma Cu$ 4. The decrease of Cu^{2+} content with increasing extent of reduction is now intermediate between the dilute specimens and pure CuO which does not produce Cu_2O (*11*). The presence of CuO is therefore reflected in the redox behavior.

DISCUSSION

1. Surface Models and Reduction Processes

The treatment of data associated the experimental quantity $(H_2O)_R$ with the amount of Cu^0, and $(H_2)_I$ with Cu^{1+}. The assumption is in analogy with the MoO_3/Al_2O_3 system where $(H_2O)_R$ and $(H_2)_I$ were found to give Mo^{4+} and Mo^{5+}, respectively, and is supported by the agreement found between the amount of Cu^0 determined from $(H_2O)_R$ and that titrated by N_2O. It is now of interest to correlate the reduction process with the surface model emerging from this and from previous studies.

The experimental evidence shows that in the as-prepared catalyst most of the Cu^{2+} ions are in octahedral positions, unlike the case of bulk $CuAl_2O_4$. This precursor state of the catalyst is hydroxylated. The dehydroxylation process taking place when outgassing is performed can be described according to the model of Knözinger and Ratnasamy (K and R) (*12*) for γ-Al_2O_3. In particular, if (110) planes are considered, two layers, designated C and D, are present, differing in the cation arrangements. In the C layer, a row of tetrahedral cations and one of octahedral cations are present, whilst in D only octahedral positions are occupied. If for the sake of simplicity the small fraction of Cu^{2+} present in tetrahedral sites is neglected, the capping OH^- ions on the C layer will be coordinated to tetrahedral Al^{3+} (Fig. 4, row n) and to octahedral Cu^{2+} and Al^{3+} (Fig. 4, row m). We will mention three aspects which may serve as a guide for the description of the dehydroxylation process. (1) K and R note that the water desorption will favor the formation of a surface vacancy on the more

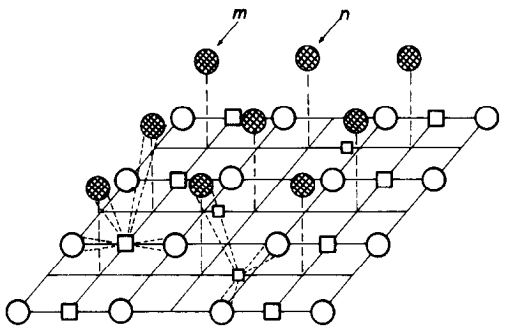

FIG. 4. A perspective of the C layer of the (110) plane. Large open circles—O^{2-} ions in the plane. Hatched circles—OH^- ions of the capping layer. Large open squares—cations in octahedral sites (Al^{3+} and Cu^{2+}). Small open squares, cations in tetrahedral sites (Al^{3+}). Rows m and n individuate OH^- capping ions coordinated to octahedral and tetrahedral cations, respectively.

negatively charged position (Ia, tetrahedral site, in K and R designation), whilst an O^{2-} ion will be left on the more positively charged position (IIb, octahedral). If applied to the surface copper spinel, this process will tend to leave CUS (coordinatively unsaturated surface) positions on tetrahedral Al^{3+}. (2) A second criterion stems from the consideration that the difference in "effective charge" between the two positions Ia and IIb ($= -0.25\,e$) is small, and more importantly can then be assumed by the chemical character of the bond. In view of its more basic character, it is reasonable to assume that OH^- is preferentially cleaved from Cu^{2+} rather than from Al^{3+}. This criterion receives support from the observation of Barber *et al.* (*13*) that no hydroxylated copper species are produced in a SIMS study of $Cu_xMg_{1-x}Al_2O_4$ solid solutions, when an easily hydrated cation (Mg^{2+}) is present. (3) Finally, geometrical considerations favor interaction between (close) OH^- groups belonging to the same row, thus leaving vacancies on both tetrahedral and octahedral rows. In the real case, if the Cu^{2+} are arranged orderly with the Al^{3+}_{oct}, the vacancies left by dehydration will be left on Al^{3+}_{tetr}. (point 1, above), or more likely will alternate with O^{2-} ions in both tetrahedral and octahedral rows. In the former case the surface coordination of copper will be of type **a**, in the second case of type **b**.

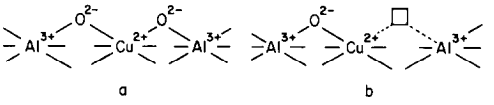

Had two or more close-lying Cu^{2+} been present in the hydroxylated surface, dehydration would have tended to expose Cu^{2+} ions, either by elimination of a water molecule within the same row (point 3), or between octahedral Cu^{2+}–OH and tetrahedral Al^{3+}–OH^- groups (point 2). Reasoning along similar lines shows that on the D layer (only octahedral ions present) the possible arrangements consist of Cu^{2+} coordinated to two O^{2-} ions or to one O^{2-} ion (plus a vacancy). Finally, on the (100) plane which is also found in $_\gamma$-Al_2O_3, the octahedral Cu^{2+} ions, after dehydration, will be either associated with one O^{2-} ion or will have a vacancy. Complete exposure of Cu^{2+} ions can also occur in principle if an "island" of Cu^{2+} ions is present.

In summary, surface Cu^{2+} ions will be either coordinated to two O^{2-} ions, or to one O^{2-} and one □, or to one O^{2-}, or fully exposed, the latter case being more probable when domains of copper ions are present.

The chemistry of the reduction process involves activation of the hydrogen molecule eventually leading to reductive chemisorption. An intermediate stage can be the heterolytic dissociation. In contrast to pure copper oxides, it has been reported that the Cu^{2+}/Al_2O_3 system does not show autocatalytic effects during reduction (*11*). It was also found in this laboratory that the two systems $_\gamma$-Al_2O_3 and $Cu^{n+}/_\gamma$-Al_2O_3 (n = 0, 1, 2) show comparable activity for the equilibration reaction $H_2 + D_2 = 2HD$ at low temperature. These results point to a predominant role of the support in the hydrogen activation step. Once activated, the hydrogen atoms can be reductively bonded in the proximity of Cu^{2+} ions, giving rise to

configurations exemplified by **c**, **d**, and **e** below. Further reduction of Cu^{1+} can take place, but some configurations require the

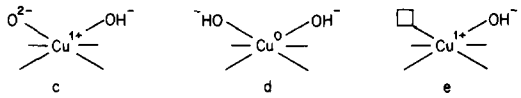

c d e

participation of O^{2-} ions below the capping layer, and/or Cu^{2+} ions in special configurations (e.g., low-coordination sites). It was already reported that the reducibility of Cu^{2+}/Al_2O_3 is much lower than that of pure copper oxides (*11*). The reduction of $CuAl_2O_4$ is thermodynamically favorable (see below) and therefore a kinetic hindrance must be assumed. We think that configurations such as **d** which easily desorb water (originating H_2O_R), are those which witness complete reduction to Cu^0. Configurations such as **c** or **e** do not lose H_2O easily, but on the other hand are less prone to pick up a further H atom; they therefore tend to maintain the oxidation state 1+. As shown in the scheme, they are associated with a strongly bound hydrogen which will desorb as water only at high temperature, yielding H_{2_t}. Any easily desorbed hydrogen either stems from heterolytic dissociation which has not proceeded to the reductive chemisorption, or from an easily reversible redox chemisorption not measured by the present procedure.

A few comments can be made with regard to the conclusion that initial activation of hydrogen does not proceed on copper, but that the activated hydrogen must be able to interact successively with copper ions. This hypothesis can be effectively described as a special case of spillover. The phenomenon has been recently reviewed by Dowden (*14*), who also gives the appropriate rationalization of the phenomenon in thermodynamic terms. It is therefore possible to use Dowden's treatment as a guideline also in the present case. In spillover, adsorption on a "bad" adsorber is finally achieved through a precursor adsorption on a "good" adsorption site. Usually, but not necessarily, the "bad" and "good" sites belong to different phases. The "good" adsorbing site will involve special configurations, such as CUS Al^{3+} ions, close to edges or to other defects. This situation implies a smaller Madelung energy of the site, and a polarization action favoring the heterolytic dissociation $H^-{-}{-}{-}H^+$ (formal charges indicated). As pointed out by Dowden, when charged particles are involved the total spillover process will occur more easily if both positive and negative particles migrate. In the present case, this requirement favors the migration of the whole complex $H^-{-}{-}{-}H^+$; hence the preservation of a molecular identity. Migration will be assisted by the existence in the immediate neighborhood of Cu^{2+}–O^{2-} couples or of a Cu^{2+}–O^{2-}–Cu^{2+} configuration. In fact the O^{2-} ions, in view of their bonding to copper, are more basic and interact favorably with H^+, whilst the H^- moiety will be able to interact with one or two Cu^{2+} ions reducing it to Cu^0 in the former case, and to $2Cu^{1+}$ ions in the second case. One can see that the energetics of the process requires special configurations, and migration over short distances. It can also be understood that eventually the reduction will be kinetically hindered.

In summary, the local configuration will greatly affect the kinetic evolution of the reduction process, simulating a stable state, or a quasi equilibrium for the supported system. The meaning of Figs. 2 and 3 is thereby emphasized. They are operational diagrams, and the independence of the oxidation state distribution on initial Cu^{2+} concentration (Fig. 2) shows that at low copper loadings the relative concentrations of different configurations are very similar, whilst at high loading (Fig. 3) the situation is different, domains of Cu^{2+} ions are found, giving rise to a different average distribution.

2. *Statistical Model and Thermodynamics of Reduction*

If the true equilibrium state were reached under operating conditions, complete reduction to Cu^0 should be observed. The re-

duction is slowed down so effectively that a quasi-equilibrium state is reached, since it is little influenced by operationally feasible time. In a first approach, and as an extreme approximation, we could then ignore the thermodynamic aspects, and treat the problem as a purely statistical one, in which there is no role played by the energy of reduction to Cu(I) or Cu(0).

The Cu^{2+} ions will undergo reduction if they pick up one or (at most) two electrons each from the hydrogen atoms. The hypothesis that the determining step is actually an activation of H atoms means that a pool of activated H atoms is made available for the reduction process. If we assume that the interaction with the pool of activated H atoms is purely statistical, each Cu^{2+} ion will interact with zero, one, or two H atoms with equal probability. As a consequence, it will correspondingly stay as Cu^{2+}, or evolve to Cu^{1+} or to Cu^0. The problem is therefore to calculate the most probable statistical distribution of a given number of H atoms, h in total, among a given number of Cu^{2+} ions, c in total, yielding Cu^{2+} (c_2 in number) or Cu^{1+} (c_1 in number) or finally Cu^0 (c_0 in number).

The following relations hold:

$$c = c_0 + c_1 + c_2, \tag{3}$$

$$h = c_1 + 2c_0. \tag{4}$$

From (4) one has the total number of Cu^{2+} which underwent a reduction process, which is $c_1 + c_0 = h - c_0$. If the process is a statistical one, one can state that there are s' ways to choose $c_1 + c_0$ ions out of c, where

$$s' = \binom{c}{c_1 + c_0} = \binom{c}{h - c_0}. \tag{5}$$

Among the total number of ions which underwent a reduction one can choose at random the c_0 ions which picked up two electrons in s'' ways, where

$$s'' = \binom{c_1 + c_0}{c_0} = \binom{h - c_0}{c_0}. \tag{6}$$

The total number of ways by which a given distribution $c_0 + c_1 + c_2$ can be realized is then $s' \times s''$. The probability, P, of having a given distribution will be

$$P = \frac{\binom{c}{h - c_0}\binom{h - c_0}{c_0}}{\sum_{c_0=0}^{h/2}\binom{c}{h - c_0}\binom{h - c_0}{c_0}} = \frac{w}{\sum_{c_0=0}^{h/2} w}, \tag{7}$$

where the denominator gives the sum of ways by which all configurations can be realized, by letting the running index c_0 assume all values from 0 to $h/2$. (if h is odd, the upper limit should be $(h - 1)/2$, but dealing with large numbers the limit can be taken as $h/2$).

To obtain the most probable distribution we make P a maximum as a function of c_0, subject to the condition $0 \leq c_0 \leq h/2$. When the values c and h are fixed, the denominator of (7) is a constant; hence the maximum for w must be looked for, and this is conveniently done by working with $\log w$. Using Stirling's approximation, and putting $d \log w/d c_0 = 0$, one obtains for $x_0 = c_0/c$ (molar fraction of Cu^0 relative to the total number of copper moles) the expression

$$x_0 = \tfrac{1}{6}(1 + 3r - (1 + 6r - 3r^2)^{1/2}), \tag{8}$$

where $r = h/c$ is the parameter which can be directly determined by adsorption measurements; from Eqs. (3) and (4), both divided by c, one has

$$1 = x_0 + x_1 + x_2, \tag{3'}$$

$$r = x_1 + 2x_0. \tag{4'}$$

By inserting different values of r in (8), one has the corresponding values of x. The resulting plot is represented in Fig. 5, curve a.

The agreement with the experimental data (heavy broken line) is poor except at low r values. The model evidently underestimates the stability of Cu^{1+} and overweights the stability of Cu^0. Hence, any model which renders the passage from Cu^{1+} to Cu^0 more difficult will improve the agreement between calculated and observed x values.

Let us now consider the physical meaning of our initial assumption, of a purely statistical distribution. It was noted that the

assumption meant that the hydrogen atoms responsible for the reduction of Cu^{2+} could distribute themselves at random. We can express this fact by the equation

$$Cu^0(H_2) + Cu^{2+} \rightleftarrows 2Cu^{1+}(H), \qquad (9)$$

where $Cu^0(H_2)$ and $Cu^{1+}(H)$ indicate a copper-containing site which has interacted with two or one H atom, respectively. The assumption of a random distribution amounts to saying that the equilibrium constant K for reaction (9) is unity. In fact, adopting the same notation employed before, one has

$$K = \frac{c_1^2}{c_0 c_2} = \frac{(h - 2c_0)}{c_0(c + c_0 - h)}, \qquad (10)$$

where from putting $K = 1$, one can obtain for x_0 the same expression (8) derived statistically. The need for giving Cu^{1+} more weight and less weight to Cu^0 means that K is larger than unity.

The general expression for x_0 can be derived from (10) to be

$$x_0 = \frac{[K + r(4 - K)] - \{[r(4 - K) + K]^2 - 4r^2(4 - K)\}^{1/2}}{2(4 - K)}$$

The result for x_0, x_1, and x_2 obtained as a function of the extent of reduction $r = h/c$ is illustrated in Fig. 5 for the values $K = 10$ (curves b) and $K = 100$ (curves c) in addition to the already mentioned curves a corresponding to $K = 1$. Curves for $K > 100$ are not reported for the sake of clarity, but the trend is evident.

The thermodynamic estimate of the equilibrium (9) referred to the aluminates, and

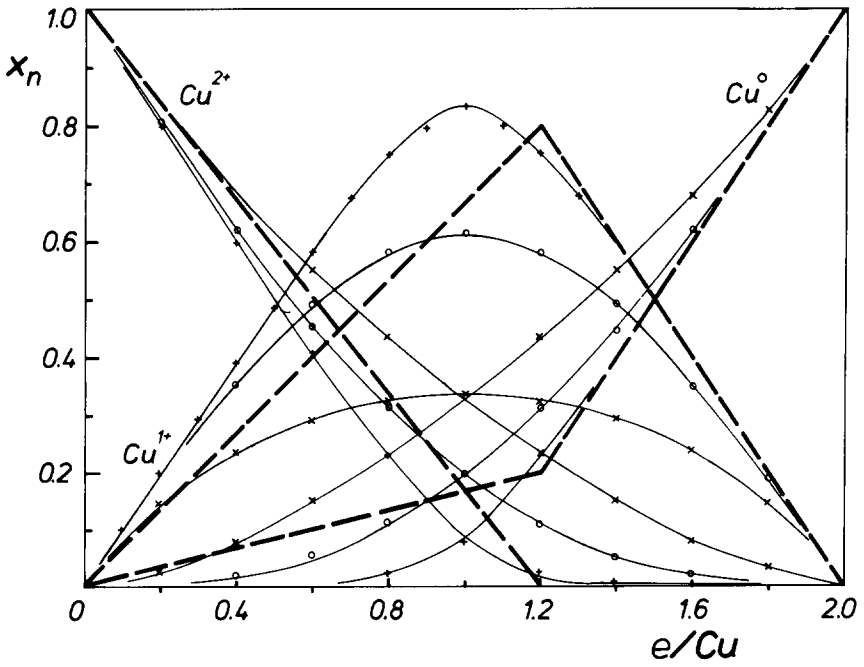

FIG. 5. A comparison of calculated molar fractions x_n of Cu^{n+} ($n = 0, 1, 2$) vs extent of reduction e/Cu, with observed values for A_yCu 2 and A_yCu 4. The observed values are shown as heavy broken lines. The key to calculated values (solid lines) is: (a) ×——×, $K = 1$; (b) ○——○, $K = 10$; (c) +——+, $K = 100$, with K equilibrium constant of reaction (9′) (see text).

hence to the equilibrium

$$Cu^0 + CuAl_2O_4 \rightleftarrows Cu_2Al_2O_4 \qquad (9')$$

(see Appendix) gives $\Delta G^\circ_{500} = -12.2$; $\Delta G^\circ_{1000} = -6.4$ (kcal/mole) where the suffix refers to the absolute temperature. Correspondingly, the following K values are calculated: $K_{500} = 2.2 \times 10^{+5}$, $K_{1000} = 25$.

These thermodynamic considerations assist us in commenting on the results illustrated in Fig. 2 where the experimental points were plotted. It was already emphasized that the diagram is not a representation of an isothermal process; hence it cannot be related simply to distribution curves computed by isothermal equilibrium states. The diagram represents a description of a surface situation developing with increasing reduction. But in order to achieve increasing extent of reduction it is necessary to increase the temperature. If we look at the diagram of Fig. 5 in the range of high H/Cu ratios (>1.2) we can see that the curves drawn for $K = 100$ closely follow the experimental values. This is the range explored at a reduction temperature of 300°C. A large K value is indeed thermodynamically expected, although a precise value cannot be assigned as specified in the Appendix. What we can say is that as far as equilibrium (9′) is concerned, it is practically reached in the large extent of reduction. However, if the low H/Cu ratio is considered, curves for large K values are ruled out. In fact, the low H/Cu ratios (<0.4) seem to agree with the $K = 1$ curves, i.e., a statistical reduction far from equilibrium. Intermediate stages of reduction ($0.4 \leq$ H/Cu ≤ 1.2) are less easily described, though the approach to high K values is apparent.

A rationalization of the whole reduction process can now be attempted. Mild reduction treatment yielding only low e/Cu ratios, leads to states far from equilibrium which can be approximated by a statistical distribution of H atoms, and hence of electrons among the sites containing Cu^{2+} ions. Further reduction is hindered for kinetic reasons. The configurations to which the Cu^{2+} ions belong play an important role in favoring the reduction process, but at low loading (≤ 4 at.% in our case) the distribution of configuration is insensitive to loading. Higher extents of reduction require more drastic treatment, and the equilibrium among Cu(0), Cu(I), and Cu(II) is approached. Up to high temperatures (about 500°C) we still have a metastable state, since complete reduction to Cu(0) is not obtained. The role of Al_2O_3 in maintaining this metastable state is apparent, and may also be of importance in more complex Cu-based systems. Finally, if the copper loading is high (when CuO appears, and possibly also when large domains containing only Cu^{2+} cations are present) the behavior is different (see Fig. 2) and it is essentially close to that of the pure copper oxides. Under these conditions, only a small fraction of Cu^{2+} undergoes a protective action by the support.

APPENDIX: RELEVANT THERMODYNAMIC DATA FOR THE $CuAl_2O_4$ SYSTEM

The relative stability of Cu(0), Cu(I), and Cu(II) can be measured by the standard free-energy change, δG°_T, of the reaction:

$$Cu(0) + Cu(II) = 2Cu(I) \qquad (1A)$$

which for the oxides and for the aluminates becomes

$$Cu + CuO = Cu_2O, \qquad (2A)$$

$$Cu + CuAl_2O_4 = Cu_2Al_2O_4. \qquad (3A)$$

The case of reaction (2A) can be easily treated since the relevant data exist in the literature. For example, following Kellogg who tabulates internally consistent data (*15*) the values reported in Table 1A are obtained.

The case of reaction (3A) is less straightforward since the relevant data must be calculated from solid electrolyte emf studies. It is important to attain internal consistency, and the recent data of Jacob and Alcock (*16*) are chosen. Other authors also give data consistent at high temperature,

TABLE 1A

ΔG°_T Values (kcal/mole) for Some Reactions Relevant to Copper–Alumina Systems

	Reaction	ΔG°_{500}	ΔG°_{1000}
(1)	$2Cu + \frac{1}{2}O_2 = Cu_2O$	-31.6^a -31.6^b	-22.8 -23.0
(2)	$Cu_2O + \frac{1}{2}O_2 = 2CuO$	-20.7^a -20.0^c -19.4^b	-8.8 -8.7 -8.7
(3)	$Cu + \frac{1}{2}O_2 = CuO$	-26.2^a	-15.8
(4)	$Cu_2O + Al_2O_3 = 2CuAlO_2$	-4.4^c $(+2.1)^b$	-3.2 (-2.9)
(5)	$CuO + Al_2O_3 = CuAl_2O_4$	$+1.9^c$ $(+2.8)^b$	-0.6 (-3.5)
(6)	$2Cu + \frac{1}{2}O_2 + Al_2O_3 = 2CuAlO_2$	-36.0^c -29.5^b	-26.2 -25.7
(7)	$Cu + \frac{1}{2}O_2 + Al_2O_3 = CuAl_2O_4$	$(-24.3)^c$ $(-23.5)^b$	(-16.4) (-19.3)
(8)	$2CuAlO_2 + \frac{1}{2}O_2 + Al_2O_3 + Al_2O_3 = 2CuAl_2O_4$	-11.7^c -17.4^b	-13.4 -12.8
(9)	$Cu + CuAl_2O_4 = 2CuAlO_2$	$(-12.2)^c$ $(-6.1)^b$	$(-6.4)^c$ $(-6.5)^b$

Note. The ΔG°_T values for the copper–alumina systems written in parentheses have been calculated from specified references ((*16*) or (*17*)) as follows (equation number given): (7) = (3) + (5); 2 × (9) = (6) − (8). Equation (2) calculated from Ref. (*16*) or (*17*) gives good agreement with review data of Ref. (*15*). The agreement for all reactions is in general good at 1000 K, near the temperature range where the measurements were taken.

[a] Ref. (*15*).
[b] Ref. (*17*).
[c] Ref. (*16*).

but diverging at lower temperature. As an illustration, the data deduced from the work of Slobodyanyuk *et al.* (*17*) are included. The set of interdependent equations of interest for the copper aluminates and copper oxide systems is summarized in the table. Note that Eq. (3A) is shifted to the right whichever value of ΔG°_T from the table is taken.

ACKNOWLEDGMENTS

We are indebted to Professor S. Carrà for clarifying discussions on thermodynamic aspects and to Dr. M. Cini for discussions on the statistical treatment. We also acknowledge the help given by Mr. G. Minelli in performing the chemical analyses. This work was supported by the project "Chimica Fine e Secondaria" of CNR (Rome).

REFERENCES

1. Friedman, R. M., Freeman, J. J., and Lytle, F. W., *J. Catal.* **55,** 10 (1978).
2. Ertl, G., Hierl, R., Knözinger, H., Thiele, N., and Urbach, H. P., *Appl. Surf. Sci.* **5,** 49 (1980).
3. Herman, R. G., Klier, K., Simmons, G. W., Finn, B. P., Bulko, J. B., and Kobylinski, T. P., *J. Catal.* **56,** 407 (1979).
4. Hall, W. K., and Lo Jacono, M., *in* "Proceedings, 6th International Congress on Catalysis, London, 1976" (G. C. Bond, P. B. Wells, and F. C. Tompkins, Eds.), Vol. 1, p. 246. The Chemical Society, London, 1977.
5. (*a*) Delorme, C., *Bull. Soc. Fr. Mineral. Cristallogr.* **81,** 79 (1958). (*b*) Pepe, F., Porta, P., and Schiavello, M., *in* "Proceedings, 8th Int. Symp. React. Solids, Gotenborgh, 1976," Vol. VI, p. 183. Plenum, New York, 1977.
6. McIver, D. S., Tobin, H. H., and Barth, R. T., *J. Catal.* **2,** 485 (1963).
7. Hall, W. K., and Massoth, F. E., *J. Catal.* **34,** 41 (1974).
8. Osinga, Th.J., Linsen, B. G., and Van Beek, W. P., *J. Catal.* **7,** 277 (1967).
9. Lo Jacono, M., Schiavello, M., and Cimino, A., *J. Phys. Chem.* **75,** 1045 (1971).
10. Freeman, J. J., and Friedman, R. M., *J. Chem. Soc. Faraday Trans. 1,* 758 (1978).
11. Voge, H. H., and Atkins, L. T., *J. Catal.* **1,** 171 (1962).
12. Knözinger, H., and Ratnasamy, P., *Catal. Rev. Sci. Eng.* **17,** 31 (1978).
13. Barber, M., Sharpe, P. K., and Vickerman, J. C., *J. Catal.* **41,** 240 (1976).
14. Dowden, D. A., *in* "Catalysis," Vol. 3, p. 136. Specialist Periodical Reports, The Chemical Society, London, 1980.
15. Kellogg, H. H., *J. Chem. Eng. Data* **14,** 41 (1969).
16. Jacob, K. T., and Alcock, C. B., *J. Amer. Ceram. Soc.* **58,** 192 (1972).
17. Slobodyanyuk, A. A., Tretyakov, Yu.D., and Bessonov, A. F., *Russ. J. Phys. Chem.* **45**(7), 1069 (1971).
18. Goodenough, J. B., "Magnetism and the Chemical Bond," Table VIII, 106. Interscience, New York, 1963.